Probing treatment response of glutaminolytic prostate cancer cells to natural drugs with hyperpolarized [5-13C]glutamine

Probing treatment response of glutaminolytic prostate cancer cells to natural drugs with hyperpolarized [5-^{13}C]glutamine

Carolina Canapè,[1] Giuseppina Catanzaro,[2] EnzoTerreno,[1] Magnus Karlsson,[3] Mathilde Hauge Lerche,[3] and Pernille Rose Jensen[3*]

1: Department of Molecular Biotechnology and Health Sciences, Molecular Imaging Center, University of Torino, Via Nizza 52, 10126 - Torino (Italy)
2: Centro Ricerche Bracco, Bracco Imaging Spa, via Ribes 5, 10010 Colleretto Giacosa (TO), Italy
3: Albeda Research Aps, Gamle Carlsberg Vej 10, 1799 Copenhagen, Denmark.

*Correspondence to: Pernille Rose Jensen, Albeda Research Aps, Gamle Carlsberg Vej 10, 1799 Copenhagen, Denmark, E-mail: pernille.rose.jensen@albeda.dk

Keywords: ^{13}C NMR, DNP, hyperpolarization; prostate cancer; resveratrol; sulforaphane; treatment

Word count: 4923 (5000 allowed)

Abstract (200 words)

Purpose: The correlation between glutamine metabolism and oncogene expression in cancers has lead to a renewed interest in the role of glutamine in cancer cell survival. Hyperpolarized [5-^{13}C]glutamine is evaluated as a potential biomarker for non-invasive metabolic measurements of drug response in prostate cancer cells.

Methods: Hyperpolarized [5-^{13}C]glutamine is used to measure glutamine metabolism in two prostate cancer cell lines (PC3 and DU145) before and after treatment with the two natural anticancer drugs resveratrol and sulforaphane. An invasive biochemical assay simulating the hyperpolarized experiment is used to independently quantify glutamine metabolism.

Results: Glutamine metabolism is found to be 4 times higher in the more glutaminolytic DU145 cells compared to PC3 cells under proliferating growth conditions by using hyperpolarized [5-^{13}C]glutamine as a noninvasive probe. A significant decrease in glutamine metabolism occurs upon apoptotic response to treatment with resveratrol and sulforaphane.

Conclusion: Hyperpolarized NMR using [5-^{13}C]glutamine as a probe permits the noninvasive observation of glutaminolysis in different cell lines and under different treatment conditions. Hyperpolarized [5-^{13}C]glutamine metabolism thus is a promising biomarker for the non-invasive detection of tumor response to treatment, as it directly monitors one of the hallmarks in cancer metabolism - glutaminolysis - in living cells.

Word count: 196

Abbreviations

AUC, Area under the curve; CAD, Caspase-Activated DNase; DNP, dynamic nuclear polarization; DON, 6-diazo-5-oxo-L-Norleucine; DU145; (DU 145), Human prostate adenocarcinoma cell line; GLS, glutaminase enzyme (EC 3.5.1.2); LDH, Lactate; MTT, 3-(4,5-dimethylthiazol-2-yl)diphenyltetrazolium bromide; mU, enzyme unit, nano mole substrate converted per minute; NAD+, Nicotinamide adenine dinucleotide oxidized form; NADH, Nicotinamide adenine dinucleotide reduced form; OPA, *o*-Phthalaldehyde; Ox063, trityl radical; PC3, (PC-3) Human prostate adenocarcinoma cell line; Q, glutamine; RSV, resveratrol; SFN, sulforaphane;

Introduction

Prostate cancer is the second most common cause of cancer-related death among men in developed countries, second only to lung cancer (1). Clinical management of prostate cancer, however, remains difficult due to the biological diversity of prostate cancers. This diversity necessitates highly varied treatment approaches, ranging from active surveillance to radiation therapy and surgical removal (2,3), often with adverse side effects (4). Prostate cancer cells are only modestly responsive to the cytotoxic effects of currently available chemotherapeutic agents. Increased concentrations of these cytotoxic drugs fail to improve the response to clinical treatments and can lead to resistance to apoptosis in prostate cancer cells (5). Toxicity to normal cells is an important issue in selection of therapies and one possible strategy evaluates natural compounds that display cancer-specific cytotoxicity (6). Resveratrol and sulforaphane are two examples of natural compounds that have attracted attention for their selective toxicity to cancer cells and for their ability to sensitize cancer cells to other therapies (7,8). Both Resveratrol and sulforaphane have been shown to inhibit growth and induce apoptosis in tumor cells as well as in tumor animal models (9-12). Sulforaphane is in clinical trial phase II treating patients with recurrent prostate cancer (13). While resveratrol has not yet been in clinical trials, phamacokinetic studies in humans have been performed paving the road for testing its anti-carcinogenic effects in humans (14).

Metabolic hallmarks of cancer cells may lead to the identification of biomarkers needed for the evaluation and development of prostate cancer therapies. In addition to increased glycolysis, cancer cells often show increased lipogenesis and glutamine metabolism (15). Catabolism of glutamine (glutaminolysis) takes place in all proliferating cells, but certain cancer cells exhibit a particular glutaminolytic phenotype that makes them highly dependent on glutamine for energy production 16). Cell proliferation and metabolism are tightly linked cellular processes. For some cancer cells, activation of the phosphoinositide 3-kinase (PI3K) signalling pathway is instrumental in causing increased levels of glucose uptake and leading to a significant up regulation of cellular glucose metabolism. In other cancer cells, the same signalling pathway leads to an inefficient glutamine metabolism rather than an excess glucose metabolism (17). The latter types of cancer cells cannot survive, when there is not enough extra glutamine and are therefore said to be "addicted" to glutamine (17). Both resveratrol and sulphoraphane have been shown to act via the PI3K signalling pathway (12,13, 18). PI3K occupies a central role in several cellular processes critical for cancer progression, including metabolism, growth, survival, and motility. Among other targets PI3K regulates mTORC1, which depends on glutamine for maximal activation (17) and also the cytotoxic function of resveratrol has been correlated to the presence of glutamine during cell culturing (6). One hypothesis of this paper is thus that cellular glutaminolysis may be a biomarker for drug treatment with resveratrol and sulphoraphane.

Due to the biological diversity of prostate cancer and the lack of non-invasive clinical tools that can track tumor progression and effect of therapy, repeated invasive examinations of the patient is

currently inevitable. Technologies for non-invasive, reliable and accurate measurements of tumor progression and antitumor effects would provide a significant advance in prostate cancer treatment. To this end, a recent technological improvement in magnetic resonance (MR), hyperpolarized ^{13}C-MR (19), has radically increased the sensitivity of MR and in consequence allowed real time metabolism of ^{13}C-labeled substrates and their metabolites to be monitored in vivo (20). In particular, this new technology has proven promising in the diagnosis of cancer (21). Recently, hyperpolarized [1-^{13}C]pyruvate has been used as a biomarker for the diagnosis of prostate cancer in a clinical trial (22). Although the necessary imaging technologies are available, the development of treatment strategies for prostate cancer is challenged by the lack of relevant biomarkers predictive of treatment efficacy and useful for therapy tracking (23). Development of biomarkers that can predict response to treatments will allow improving the efficiency of therapies or help avoid unnecessary treatments, while facilitating the evaluation of potential novel breakthrough therapies.

In the current study, we evaluate noninvasive observations of glutamine metabolism as a biomarker for the treatment of prostate cancer cells. Hyperpolarized ^{13}C NMR measurements were used to probe the metabolic conversion of hyperpolarized [5-^{13}C]glutamine to [5-^{13}C]glutamate in aggressive living prostate cancer cell lines (DU145 and PC3). Noninvasive tracking of glutaminolysis shows differences in the glutamine metabolism between DU145 and PC3 cells. In agreement with the high glutaminolytic activity, both cell lines only proliferate in the presence of glutamine in the medium, thus showing that glutamine metabolism is a significant substrate for both DU145 and PC3 cells. Glutaminolysis was ~4fold higher in DU145 cells, as validated by disruptive assays. The different glutaminolytic activity of both prostate cancer cell lines was further tracked upon exposure to two natural anticancer agents, resveratrol and sulforaphane. Treatment with both drugs was more effective in the more glutaminolytic cell line DU145. Thus, noninvasive observations of glutamine metabolism are prospective biomarkers for cell line specific differences in glutamine metabolism and response to therapy.

Methods

Cell culture and treatments

DU145 and PC3 cells (America Tissue Culture Collection) were initially cultured in RPMI 1640 medium with 10% FBS, 100 units/ml penicillin, 100 µg/ml streptomycin, 2 g/L glucose, and 0.3 g/L L-glutamine (Sigma-Aldrich, St. Louis, MO, USA) at 37°C in a 5% CO_2 atmosphere. For cell experiments, DMEM low glucose medium (with or without glutamine) was supplemented with 10% FBS, 100 units/ml penicillin, 100 µg/ml streptomycin and 2 g/L sodium bicarbonate. The glucose concentration in DMEM low glucose media was increased up to 2 g/L glucose by adding the proper volume of D-(+)-Glucose solution of 100 g/L (Sigma-Aldrich). For cell counting experiments, cells were plated in 24 multi well plates at cell densities of $1.5x10^4$/well and $3x10^4$/well for DU145 and PC3 cells, respectively. For MTT, Nucleosoma and ATP assays,

cells were plated in 96 multi well plates at densities of $7.5x10^3$/well and $12x10^3$/well for DU145 and PC3, respectively. For assays of glutamine metabolism, cells were grown in T75 flasks prepared by seeding $2x10^6$ cells.

Cell treatment

Resveratrol and sulforaphane were dissolved in DMSO (Sigma-Aldrich) to obtain 100 mM and 80 mM stock solutions, respectively. Cells were plated as described above in full growth media (DMEM 2 g/L glucose, 2 mM glutamine). Following 24 h attachment, the medium was discarded and serial dilutions of the two drugs prepared in growth medium were added to cells at concentrations of 25, 50, 100, 200, 300, 400 μM of resveratrol and 5, 10, 20, 40 μM of sulforaphane. Cells cultured in medium containing 0.05 % (for sulforaphane experiments) or 0.4% DMSO (for resveratrol experiments) served as control groups.

Cell counting

Once harvested by trypsination, cells were pelleted and resuspended in an appropriate volume of PBS, then diluted 1:2 with trypan blue (Sigma-Aldrich) and counted with a hemocytometer.

ATP assay

CellTiter-Glo assay was purchased from Promega (Madison, WI, USA). Measurements were made according to the manufacturer's instructions. Briefly, plates containing $25x10^3$ cells in 100 μL per well were removed from the incubator and allowed to equilibrate at room temperature for 20 minutes. An equal volume of CellTiter-Glo reagent was added directly to the wells. Plates were incubated at room temperature for 30 minutes on a shaker and luminescence was measured on a microplate reader (PerkinElmer, Waltham, MA, USA).

MTT assay

The MTT assay measures the cellular capacity to reduce 3-(4,5-dimethylthiazol-2-yl)diphenyltetrazolium bromide (Sigma-Aldrich) to blue formazan products by various oxidoreductase enzymes (24, 25). Cells were grown in 96 well plates and after removing the supernatant, 100 μL of MTT solution (0.5 mg/mL in growth media) were added to each well. After incubation for 4 h, the resultant formazan crystals were dissolved in isopropanol (100 μL) and the absorbance intensity measured by a microplate reader at 570 nm. All experiments were performed in quadruplicate, and the MTT conversion (%) was expressed as a percentage relative to the control cells.

Nucleosome ELISA

Nucleosome Cell Death ELISA kit was acquired by Roche Applied Sciences (Germany) and used according to the instructions. Cells were grown as described above in 96 multiwell plates. After 24 h of resveratrol or sulforaphane treatments, cells were lysed with the lysis buffer supplied in the kit. Lysed cells were pelleted with a 200 *g* centrifugation for 10 minutes. 20 µL of supernatants were incubated in ELISA wells with 80 µL immunoreagent per well. ELISA assays were quantified at a detection wavelength of 405 nm. The enrichment of mono- and oligonucleosomes released into the cytoplasm of cell lysates was detected by biotinylated anti-histone- and peroxidase-coupled anti-DNA-antibodies and was calculated as follows, enrichment factor = absorbance of sample cells/absorbance of control cells. Both sample and control values were first corrected by subtracting the blank absorbance. Enrichment factor was used as a parameter of apoptosis (26) and is given as the mean ± SD of three independent experiments performed in triplicate.

Metabolic conversion of glutamine with RP-HPLC assay

Cells were grown in T75 flasks, harvested and assessed for viability by trypan blue exclusion. For lyzed cells, the harvested cells were submitted to three rounds of freeze-thawing at -80 °C before continuing with the assay. After centrifugation, cells were suspended by adding 225 µL 0.1 M NaH_2PO_4 pH 7.5, 15 µL 100 mM Norvaline (internal concentration reference) and 60 µL 100 mM Glutamine (or 60 µL H_2O in blank samples). Samples containing 0.5 million cells were incubated for 30 minutes at 37°C, then 150 µL 6% perchloric acid were added to stop the reaction and samples were put on ice for 15 min. Finally, 14 µL saturated K_2CO_3 were added to re-equilibrate pH and samples were pelleted at 15000 g for 15 min at 4°C. Supernatants were filtered with 0.2 µm PVDF syringe filter and analysed by reverse-phase HPLC as described (27). No de-amidation of glutamine is occurring using this mild protein denaturing procedure allowing the determination of glutamate concentrations. Three replicates for blanks and samples were prepared for each condition.

In vitro hyperpolarized

^{13}C-NMR polarization medium was prepared as described (28). In brief, Ox063 radical (Albeda Research, Denmark) and the gadolinium complex Gadoteridol (Bracco Imaging Spa, Italy) were dissolved to 35 mM and 4 mM, respectively, in anhydrous DMSO. Cesium hydroxide monohydrate (42.0 mg, 0.25 mmol) and [5-^{13}C]glutamine (35.3 mg, 0.24 mmol) (Cambridge Isotope Laboratories, Tewksbury, USA) were weighed into a microcentrifuge tube. The two solids were briefly whirl-mixed and polarization medium (52 µL, 57.5 mg) was added. The resulting slurry was sonicated and whirl-mixed until a solution was obtained. The approximate density of the liquid sample was ~1.5 g/mL and the resulting concentrations were: Ox063 radical 20 mM, gadolinium 2.3 mM and ^{13}C 2.7 M. 30 µmol of a [5-^{13}C]glutamine sample prepared according to the protocol described above were hyperpolarized and dissolved in 5 mL 40 mM phosphate

buffer pH 7.0 with addition of HCl to neutralize the base. The pH after dissolution was 7.1. The sample was hyperpolarized under DNP conditions at 1.2 K and 3.35 T in a prototype polarizer (19). For cellular NMR assays, cells were harvested by trypsinization and counted. Cell viability was assessed with trypan blue exclusion. 10 million cells were dissolved in 500 μl 40 mM phosphate buffer of pH 7.3 and placed in a flat bottom 10 mm NMR tube adjusted in the NMR spinner to cover the active volume. The sample tube, with a connected inlet tubing, was placed into a 14.1 T magnet and equilibrated for 5 minutes at 310 K. 1 ml of the dissolved hyperpolarized [5-^{13}C]glutamine was injected through the tubing, resulting in a glutamine concentration of 3.5 mM in the cell suspension. A time series was acquired by applying a 20 degree pulse every 2 s and 48 time points were recorded. The acquisition was started just before the injection of the hyperpolarized [5-^{13}C]glutamine.

Kinetic fitting

The data from the data sets containing the signals from glutamine and glutamate were first corrected for the effect of pulsing by dividing the data sets with $\cos(a)^n$ where a is the flip angle (20°) and n is the pulse ordinal number. The corrected data were then fitted to the following two differential equations:

1) $dS/dt = -k*S(t) - 1/T1_S*S(t)$

2) $dP/dt = k*S(t) - 1/T1_P*P(t)$

Here, S denotes the signal from substrate glutamine, $T1_S$ denoted the T_1 of glutamine, P denotes the signal from glutamate and $T1_P$ denotes the T_1 of glutamate. The T_1 of glutamine was determined from the decay of the substrate signal (20 ± 2 s). The T_1 of glutamate was fitted to 24 ± 2 s. All fitted curves had a coefficient of determination R^2 above 0.91.

Data Analysis

Each experiment was repeated at least in triplicate and means ± SD for each value were calculated. Statistical analysis of the results was performed using the Student's t-test and one-way ANOVA, followed by Dunnett's

multiple comparison test. Significant differences are indicated with "*" ($P<0.05$) in all figures. All the statistical analyses were performed using the statistical package GraphPad Prism. Spectral analysis was performed using the software MNova (Mestrelab Research, Santiago de Compostela, Spain).

Results

Glutamine addiction of prostate cancer cells

PC3 and DU145 are widely used aggressive human prostate cancer cell lines derived from different origin. Both cell lines have been shown to exhibit a strong dependence on glutamine for proliferation (29,30). This dependence may be connected to a glutaminolytic phenotype of the cell type. Cell growth characteristics were evaluated for PC3 and DU145 cell lines to compare their dependence on glutamine for growth (degree of glutamine addiction). Figure 1 shows the growth of DU145 and PC3 cells in the absence and in the presence of glutamine, as evaluated by the cell number and cell viability (MTT conversion). The growth of both cell lines was diminished by glutamine withdrawal in a time-dependent manner. A significant decrease of cell proliferation was reached after 72 h of glutamine withdrawal ($P<0.05$) in both cell types (Figure 1(A,B)). Glutamine depletion affected MTT conversion relative to the decrease in cell number in both cell lines as shown in Figure 1(C,D). In DU145 cells, MTT conversion significantly decreased by 36 ± 1.2 % already after 24 h ($P<0.05$), while in PC3 cells MTT conversion significantly decreased (by 28 ± 0.77 %) only after 48 h ($P<0.05$). ATP levels in the two cell types were measured to evaluate, if the cell proliferation arrest occurred as a result of reduced mitochondrial activity. Cellular ATP was strongly reduced in DU145 cells during glutamine restriction relative to control conditions (by 77,7 ± 1.5% at 48 h and 79.4 ± 2.1 % at 96 h), while it was moderately diminished in PC3 (by 29.7 ± 1.03% at 48 h and 34.9 ± 5.9 % at 96 h). Glutamine depletion is clearly able to introduce proliferation arrest in PC3 and DU145 cells, thus underlining the importance of this metabolic pathway for both cell types to propagate.

In order to noninvasively probe glutamine metabolism in real time with hyperpolarized [5-^{13}C]glutamine in prostate cancer cells, a protocol was adapted that we developed previously for liver cancer cells (28). [5-^{13}C]glutamine was polarized to approximately 30 % in the solid state. The final concentration of the substrate in the NMR tube was 4 mM. Figure 2A displays the hyperpolarized ^{13}C NMR experiment after injection of [5-^{13}C]glutamine into a cell suspension of DU145 cells. A time series of 1D ^{13}C NMR spectra shows the build-up of the metabolic product signal ([5-^{13}C]glutamate) and the decay of a signal with similar chemical shift originating from [1-^{13}C]pyroglutamate,. The pyroglutamate signal is not a result of metabolism, but results from a chemical impurity present in commercially available [5-^{13}C]glutamine (28). A ^{13}C NMR spectrum of the cell suspension taken 20 seconds after injection of hyperpolarized substrate is displayed separately in Figure 2B, showing the substrate peak from [5-^{13}C]glutamine and the natural abundance signal from the C1 of glutamine, together with the intracellular metabolite signal which is detected at a signal to noise ratio of ~75. The T_1 of [5-^{13}C]glutamine at 37 °C and 14.1 T was determined upon correction for the loss of signal due to excitation pulses to 20 ± 2 s.

Glutamine addiction correlates to glutamine metabolism in prostate cancer cells

The proliferative dependency of aggressive prostate cancer cells on glutamine availability supposedly correlates to activated oncogenes that influence glutamine catabolism (29). The first metabolic step in glutamine catabolism is its conversion to glutamate in a reaction catalyzed by the enzyme glutaminase. Glutamate forms from the hyperpolarized [5-^{13}C]glutamine probe by two catalysed steps, the cellular uptake and the glutaminase catalysed reaction. It was therefore evaluated, if hyperpolarized [5-^{13}C]glutamine metabolism is a possible biomarker for the glutamine dependence in prostate cancer cells. The formation of the metabolic product [5-^{13}C]glutamate was compared between the two prostate cancer cell types and an evaluation of the area under the curve (AUC) is shown in Figure 2D. The AUC was 37.3 ± 4.8 a.u. in DU145 cells whereas it was 9.0 ± 1.0 a.u. or approx. 4 times lower in PC3 cells. The kinetic profile is similar for the DU145 and the PC3 cells, although the latter show less product formation (Figure 2C). The decay over time of the hyperpolarized substrate ([5-^{13}C]glutamine) is identical in experiments performed with the two cell types, because the decay is dominated by relaxation rather than metabolism.

The hyperpolarization data indicating different glutamine metabolism in DU145 and PC3 cells were validated by conventional biochemical methods. To mimic the hyperpolarization protocol, glutamine was fed to whole cells ($5x10^5$) enabling a quantification of combined glutamine uptake and metabolism to glutamate. The quantification was made with RP-HPLC after disrupting the cells with perchloric acid. Production of glutamate from glutamine was determined as 30±2 and 11±4 mU/million cells, in DU145 and PC3, respectively (Figure 2E). In consequence, both the non-invasive hyperpolarized NMR assay and the disruptive assay show a 3-4-fold larger metabolism of glutamine to glutamate in DU145 cells, which are more addicted to glutamine than PC3 cells. The measured glutamine to glutamate conversion was stable under the chosen growth conditions in both cell types when measured at 48 and 96 hours.

Resveratrol and sulforaphane treatment in PC3 and DU145

DU145 and PC3 cells were exposed to increasing concentrations of resveratrol and sulforaphane to determine, if the degree of glutamine addiction is reflected in the response to drug treatment. The effect of treatment was measured in both cell types as a decrease in cell proliferation, a decrease in MTT conversion and as an induction of apoptosis (Figures 3 and 4). Dose response curves were performed to identify the appropriate drug concentration to induce apoptosis. DU145 was sensitive to resveratrol treatment, with significant apoptosis achieved at 50 μM ($p<0.05$), and a maximum of 3.5 ± 0.51-fold increase in nucleosome release into the cytoplasm obtained at 200 μM. PC3 cells were less responsive to resveratrol-induced apoptosis showing significant apoptosis with 1.8 ± 0.86-fold increase in nucleosome release into the cytoplasm, only at the highest tested concentrations (300 and 400 μM; see Figure 3F). When DU145 cell were treated with resveratrol at high concentration (400 μM, Figure 3E) this resulted in a decrease of apoptotic enrichment factor. This effect may be due apoptotic cells progressed into late apoptotic

cells (secondary necrotic cells). In this state the cell membrane becomes more permeable, resulting in the leakage of intracellular molecules such as nucleosomes release into the cytoplasm (31). Alternatively high concentration of an apoptosis-inducing stimulus could induce necrosis rather than apoptosis (32).

Antiproliferative action of resveratrol in DU145 cells resulted in a 50% reduction (IC_{50}) at 100 μM. In PC3 cells, no IC_{50} could be determined with reasonable drug concentrations (33). The MTT conversion was significantly decreased to 80.82 ± 4.06 % ($P<0.05$) at 50 μM in DU145 cells, while a significant decrease to 80.6 % was achieved in PC3 cells only at 100 μM ($P<0.05$). Similarly, the effects of sulforaphane on cell growth, MTT conversion and apoptosis in DU145 and PC3 cells are shown in Figure 4. Treating DU145 cells with 5-20 μM sulforaphane resulted in maximum nucleosome release (5.8 ± 1.7 fold increase) into the cytoplasm at 5 μM. At this concentration of sulforaphane, cell numbers and mitochondrial activities were significantly reduced to 55.0 % ($P<0.05$) and 63.3 % ($P<0.05$) of the control. In PC3 cells, apoptosis was observed in a concentration-dependent manner with a maximum of 3.17 ± 0.55 fold at 40 μM. At this concentration of sulforaphane, cell numbers and mitochondrial activities were significantly reduced to 40.0 % ($P<0.05$) and 33.4 % ($P<0.05$) of the control. Taken together, these data suggested that both drug treatments are preferentially cytotoxic to the more glutamine addictive DU145 cell type.

The potential of hyperpolarized [5-^{13}C]glutamine to non-invasively monitor the effect of drug treatment in prostate cancer cells was evaluated. Metabolic build-up curves of hyperpolarized [5-^{13}C]glutamate were acquired after administration of hyperpolarized [5-^{13}C]glutamine substrate to either DU145 control cells or cells treated with 200 μM resveratrol (Figure 5A). Areas under the curves were determined and are shown in Figure 5B. Following treatment, a decrease by 47 % ($n=3$, $P< 0.05$) in AUC was observed. The metabolic conversion of glutamine was also quantified using the RP-HPLC based biochemical assay, Figure 5C. In DU145 cells a significant decrease by 59.3 ± 4.7 % ($P<0.05$) was observed upon treatment with 200 uM resveratrol. The two assays show a similar and much reduced metabolism of glutamine to glutamate in the glutamine dependent cell type, DU145. Resveratrol treatment (200 μM) of PC3 cells resulted in a reduction in produced glutamate by 39.6 ± 2.2 % ($P<0.05$). Glutamine metabolism was similarly quantified for sulforaphane treated cells at the two concentrations with maximum apoptotic effect (5 μM for DU145 and 40 μM for PC3). Under these conditions the glutamine metabolism was significantly reduced by 55.5 ± 4.2 % ($P<0.05$) in DU145 and 50.8 ± 6.3 % ($P<0.05$) in PC3 compared to untreated cells.

A simple kinetic model was applied (see Methods section) in order to quantitatively compare hyperpolarized ^{13}C-MR and biochemical measurements of glutamine metabolism. This model allowed the extraction of the amount of hyperpolarized [5-^{13}C]glutamate produced in the two prostate cancer cell types to 210 ± 21 amol/s/cell in DU145 cells and 40 ± 10 amol/s/cell in PC3 cells. Using the same model,

hyperpolarized [5-^{13}C]glutamate formation in DU145 was determined for resveratrol treated cells as 100 ± 12 amol/s/cell.

Discussion

The glutaminolytic phenotype shared by many tumor cell types has been associated with a cellular addiction to glutamine for the maintenance of cell viability (34). Such glutamine addiction and a glutaminolytic phenotype have been reported for the human prostate carcinoma cell types, PC3 and DU145 (29,30). Our results confirmed that both cell types are highly dependent on glutamine for proliferation and showed the more aggressive prostate cancer cell type, DU145, to be more strongly dependent on glutamine for proliferation. While examples have been reported for cells with dramatically changed viability upon glutamine withdrawal (34), the prostate cancer cell types DU145 and PC3 are able to survive in glutamine deficient medium. Glutamine deprivation instead resulted in proliferation arrest and in a growth correlated decrease in MTT conversion in both prostate cancer cell types. The MTT conversion was almost halved in DU145 cells after 24 h in glutamine depleted medium (Figure 1C), while it was not significantly changed in the PC3 cells at this time point (Figure 1D), suggesting that the DU145 cells are more glutamine dependent than PC3 cells. That DU145 cells are more addicted to glutamine than PC3 cells is further supported by a time dependent increase in PC3 cell viability for cells grown in glutamine deficient medium (Figure 1D). It seems that PC3 in contrast to DU145 cells pick up over time and adapt to the glutamine free growth condition.

The higher sensitivity of DU145 cells to glutamine withdrawal was correlated to a significantly higher degree of glutaminolysis in DU145 compared to the PC3 cells, as measured by glutamine metabolism to glutamate. The metabolic conversion of hyperpolarized [5-^{13}C]glutamine to hyperpolarized [5-^{13}C]glutamate was quantified and proved to be 3-4 times higher in DU145 cells than in PC3 cells. The rates of glutamate production obtained in the hyperpolarized experiments are consistent with rates obtained by the conventional biochemical method (210 amoles/s/cell and 500 amoles/s/cell, respectively, in DU145 cells and 40 amoles/s/cell and 180 amoles/s/cell, respectively, in PC3 cells). The rates calculated from the hyperpolarized experiments are generally lower than those quantified with RP-HPLC from perchloric acid extracts. The difference in the measured rates may be related to the different conditions used in the two assays. The applied glutamine concentration, although high in both assays to ensure saturation of the transport into the cells, differ (3.5 mM and 20 mM respectively in the hyperpolarized and RP-HPLC experiments) and the assay time is much shorter in the hyperpolarized experiments (1.5 min) compared to the conventional biochemical assay (30 min).

The glutamine metabolism is in both assays measured as a result of a combination of an active cellular uptake of glutamine and as a result of glutaminase activity. A situation where the uptake of glutamine is rate limiting and different in the two cell types could explain why the reported rates obtained

with the two assays (hyperpolarized assay during 1.5 minute and conventional biochemical assay during 30 minutes) differs. In support of an uptake rate limitation in prostate cell glutaminolysis a three times increased glutamate production was measured in disrupted DU145 cells (1516 amoles/s/cell) and a two times increase in PC3 cells (360 amoles/s/cell). In general, the metabolic conversion of glutamine is high in both prostate cancer cell types. The conversion rate measured in PC3 cells is comparable to the rate recently reported for the glycolysis in PC3 cells (35). This high rate of glutamine metabolism in prostate cancer cells could be the result of an increased cellular glutamine transport, as reported for malignant hepatoma cells (36,37) and a consequence of higher glutaminase expression (29)

We exposed DU145 and PC3 cells to two well-established natural systemic drugs, resveratrol and sulforaphane, that are suggested to act on glutamine dependent cellular regulators. Metabolic response to treatment was measured for drug doses matched with maximum apoptotic effect and cellular proliferation arrest to 50%. At these drug concentrations, glutamine metabolism was approximately half of that in the untreated cells (decreased by 59.3 ± 4.7 % and 55.5 ± 4.2 % in DU145 cells using resveratrol (200 μM) and sulforaphane (5 μM), respectively and by 50.8 ± 6.3 % in PC3 cell using sulforaphane (40 μM)). The high rate of glutamine metabolism in prostate cancer cells, in particular in the highly glutaminolytic DU145 cells, made it possible to monitor and quantify hyperpolarized [5-^{13}C]glutamine metabolism also in drug treated cells. In resveratrol treated DU145 cells the rate of glutamate production obtained from hyperpolarized [5-^{13}C]glutamine was 100 amoles/s/cell, which is slightly below half of the rate measured in the untreated cells (210 amoles/s/cell). This change in glutamine metabolism upon treatment is consistent with the biochemical measurements (untreated 500 amoles/s/cell and treated 200 amoles/s/cell). The significant effect on glutamine metabolism in response to natural drugs shows that glutamine metabolism is a potentially strong indicator of the effect of this type of therapy on prostate tumour cells. The earlier response of DU145 cells to the natural drugs is consistent with a more glutaminolytic phenotype in DU145 than in PC3 cells. Resveratrol treatment did not yield effects on apoptosis and cell proliferation in PC3 cells, while a significant decrease in glutamine metabolism by 39.6 ± 2.2% was measured in PC3 cells treated with 200 µM resveratrol. The decrease in glutamine metabolism could be correlated to a decrease in mitochondrial activity. Glutamine metabolism thus could provide an early biomarker of cellular response to drug treatment that is detectable before effects upon cell proliferation and cell death can be detected.

Our interest in this study has been to evaluate hyperpolarized [5-^{13}C]glutamine metabolism to hyperpolarized [5-^{13}C]glutamate as a possible predictive biomarker for the efficacy of prostate cancer therapy. The detection of glutamine metabolism in prostate cancer with hyperpolarized [5-^{13}C]glutamine was previously unsuccessful both in animals and in cells (38, 39). We show here that the use of an improved protocol shown to work in a rat liver cancer model (28) allows us to follow hyperpolarized [5-^{13}C]glutamine metabolism in glutaminolytic prostate cancer cells.

A suitable noninvasive predictive biomarker of treatment efficacy in prostate cancer ideally should have various characteristics: The biomarker should provide significant functional contrast between prostate cancer and healthy tissue, it should correlate with a wanted effect of a therapy and it should be quantifiable in the relevant cells or tissue (23). This study shows that real time, non-invasive metabolism of hyperpolarized [5-^{13}C]glutamine meets these demands as the metabolism of a hyperpolarized [5-^{13}C]glutamine probe (i) is particularly prominent in highly glutaminolytic prostate cancer cell types, (ii) correlates to drug treatment efficacy and (iii) can be quantified in highly glutaminolytic isolated cells.

Metabolic reprogramming renders cancer cells highly dependent on specific metabolic enzymes or processes. As a predictive biomarker, glutamine metabolism offers great promise due to its central role in cancer metabolism. In consequence glutamine metabolism has previously been suggested as biomarker in tumors that fail to show high aerobic glycolysis (40). Due to the excellent resolution of magnetic resonance spectroscopy, metabolism to glutamate can be probed by hyperpolarized NMR methods. The noninvasive measurement of glutamine metabolism and its sensitivity to drug treatment, detected herein with hyperpolarized [5-^{13}C]glutamine in living prostate cancer cells, therefore potentially provides additional diagnostic and prognostic information for drug evaluation and treatment strategies in cancer.

Acknowledgement

This study has been supported in part by Regione Piemonte (POR FESR 2007/20, line I.1.1). Fabio Tedoldi, Silvio Aime, Claudia Cabella and Sebastian Meier are gratefully acknowledged for stimulating discussions.

References

1. Jemal A, Siegel R, Ward E, Hao Y, Xu J and Thun, MJ. Cancer statistics 2009. CA: A Cancer Journal for Clinicians 2009;59:225–249.

2. Epstein JI, Sanderson H, Carter HB, Scharfstein DO. Utility of saturation biopsy to predict insignificant cancer at radical prostatectomy. Urology 2005;66:356–60.

3. D'Amico AV, Chen MH, Renshaw AA, Loffredo M, Kantoff PW. Androgen suppression and radiation vs radiation alone for prostate cancer: a randomized trial. JAMA 2008;299:289–295.

4. Chen F, Zhao X. Prostate Cancer: Current Treatment and Prevention Strategies. Iran Red Cres Med J. 2013;15(4):279-84. DOI: 10.5812/ircmj.6499

5. Shankar S, Srivastava RK. Involvement of Bcl-2 family members, phosphatidylinositol 3'-kinase/AKT and mitochondrial p53 in curcumin (diferulolylmethane)-induced apoptosis in prostate cancer. Journal of oncology 2007;30:905-918.

6. Freeman MR, Kim J, Lisanti MP and Di Vizio D. A metabolic perturbation by U0126 identifies a role for glutamine in resveratrol-induced cell death. Cancer Biology & Therapy 2011;12(11):966–977.

7. Rashid A, Liu C, Sanli T, Tsiani E, Singh GT, Bristow RG, Dayes I, Lukka H, Wright J and Tsakiridis T. Resveratrol enhances prostate cancer cell response to ionizing radiation. Modulation of the AMPK, Akt and mTOR pathways. Radiation Oncology 2011;6:144-156

8. Gill C, Walsh SE, Morrissey C, Fitzpatrick JM, and Watson RWG. Resveratrol Sensitizes Androgen Independent Prostate Cancer Cells to Death-Receptor Mediated Apoptosis Through Multiple Mechanisms. The Prostate 2007;67:1641-1653.

9. Aggarwal BB, Bhardwaj A, Aggarwal RS, Seeram NP, Shishodia S, Takada Y. Role of resveratrol in prevention and therapy of cancer: preclinical and clinical studies. Anticancer Res 2004;24:2783–840.

10. Jang M, Cai L, Udeani GO, Slowing KV, Thomas CF, Beecher CW, Fong HH, Farnsworth NR, Kinghorn AD, Mehta RG, Moon RC, Pezzuto JM. Cancer chemopreventive activity of resveratrol, a natural product derived from grapes. Science 1997;275:218–20.

11. Gamet-Payrastre L, Li P, Lumeau S, Cassar G, Dupont MA, Chevolleau S, Gasc N, Tulliez J, Terce F. Sulforaphane, a naturally occurring isothiocyanate, induces cell cycle arrest and apoptosis in HT29 human colon cancer cells. Cancer Res. 2000;60:1426–1433. [PubMed: 10728709]

12. Kim JH, Kwon KH, Jung JY, Han HS, Shim JH, Oh S, Choi KH, Choi ES, Shin JA, Leem DH, Soh Y, Cho NP, Cho SD. Sulforaphane increases cyclin-dependent kinase inhibitor, p21 protein in human Sakao and Singh Page 9 oral carcinoma cells and nude mouse animal model to induce G2/M cell cycle arrest. J Clin Biochem Nutr. 2010;46:60–67. [PubMed: 20104266]

13. Alumkal JJ. The Effects of Sulforaphane in Patients With Biochemical Recurrence of Prostate Cancer. Web site. http://www.ClinicalTRials.gov Identifier NCT01228084. Published October 19, 2010. Updated July 19, 2013. Accessed February 12, 2014.

14. Gescher A, Steward WP, Brown K. Resveratrol in the management of human cancer: how strong is the clinical evidence? . Ann N Y Acad Sci. 2013 1290:12-20.

15. Zhao Y, Butler EB and Tan M. Targeting cellular metabolism to improve cancer therapeutics. Cell Death Dis. 2013;4:e532

16. DeBerardinis RJ, Mancuso A, Daikhin E, Nissim I, Yudkoff M, Wehrli S and Thompson CB. Beyond aerobic glycolysis: Transformed cells can engage in glutamine metabolism that exceeds the requirement for protein and nucleotide synthesis. PNAS 2007;104(49):19345–19350.

17. Wise DR, Thompson CB. Glutamine Addiction: A New Therapeutic Target in Cancer Trends Biochem Sci 2010; 35(8): 427–433.

18. Shankar S, Ganapathy S and Srivastava RK. Sulforaphane enhances the therapeutic potential of TRAIL in prostate cancer orthotopic model through regulation of apoptosis, metastasis, and angiogenesis. Clin Cancer Res 2008;14(21):6855-6866.

19. Ardenkjær-Larsen JH, Fridlund B, Gram A, Hansson G, Hansson L, Lerche MH, Servin R, Thaning M, Golman K. Increase in signal-to-noise ratio of >10,000 times in liquid-state NMR, PNAS 2003;100(18):10158–10163.

20. Kurhanewicz, J, Vigneron DB, Brindle K, Chekmenev EY, Comment A, Cunningham CH, DeBerardinis RJ, Green GG, Leach MO, Rajan SS, Rizi RR, Ross BD, Warren WS and Malloy CR. Analysis of cancer metabolism by imaging hyperpolarized nuclei: prospects for translation to clinical research. *Neoplasia* 2011 **13**(2), 81-97.

21. Golman K, Zandt RI, Lerche MH, Pehrson R, Ardenkjaer-Larsen JH. Metabolic imaging by hyperpolarized 13C magnetic resonance imaging for in vivo tumor diagnosis. Cancer Res 2006;66:10855–10860.

22. Nelson SJ, Kurhanewicz J, Vigneron DB et al. Metabolic imaging of patients with prostate cancer using hyperpolarized [1-13C]pyruvate, Science Translational Medicine 2013; 5(198), Article number 198ra108.

23. Madu CO and Lu Y. Novel diagnostic biomarkers for prostate cancer. *J Cancer* 2010; 1:150-177.

24. Berridge MV and Tan AS. Characterization of the Cellular Reduction of 3-(4,5-dimethylthiazol-2-yl)-2,5-diphenyltetrazolium bromide (MTT): Subcellular Localization, Substrate Dependence, and Involvement of Mitochondrial Electron Transport in MTT Reduction', Archives of Biochemistry and Biophysics, 1993; 303: 474–482.

25. Liu Y, Peterson DA, Kimura H and Schubert D. Mechanism of Cellular 3-(4,5-Dimethylthiazol-2-yl)-2,5-Diphenyltetrazolium Bromide (MTT) Reduction', Journal of Neurochemistry, 2002;69: 581–593.

26. Zeise E1, Weichenthal M, Schwarz T, Kulms D. Resistance of human melanoma cells against the death ligand TRAIL is reversed by ultraviolet-B radiation via downregulation of FLIP. J Invest Dermatol. 2004; 123(4):746-54.

27. Bartolomeo MP, Maisano F. Validation of a reversed-phase HPLC method for quantitative amino acid analysis. J Biomol Tech. 2006;17(2): 131-137.

28. Cabella C, Karlsson M, Canapè C et al. *In vivo* and *in vitro* liver cancer metabolism observed with hyperpolarized [5-13C]glutamine. J Magn Reson. 2013;232:45-52.

29. Gao P, Tchernyshyov I, Chang TC, Lee YS, Kita K, Ochi T, Zeller KI, De Marzo AM, Van Eyk JE, Mendell JT, and Dang CV. c-Myc suppression of miR-23 enhances mitochondrial glutaminase and glutamine metabolism. Nature. 2009;458(7239):762–765.

30. Liu X, Fu YM and Meadows GG. Differential effects of specific amino acid restriction on glucose metabolism, reduction/oxidation status and mitochondrial damage in DU145 and PC3 prostate cancer cells, Oncology Letters 2011; 2: 349355.

31. Poon IKH, Hulett MD, and Parish CR. Molecular mechanisms of late apoptotic/necrotic cell clearance. Cell Death and Differentiation 2010;17: 381–397.

32. Sundquist T, Moravec R, Niles A, O'Brien M, Riss T. Timing your apoptosis assays. CELL NOTES 2006;16: 18-21.

33. Udingwe CC, Ramprasath VR, Aluko RE and Jones PJH. Potential of resveratrol in anticancer and anti-inflammatory therapy. Nutr. Rev. 2008; 66(8): 445-454.

34. Wise DR, DeBerardinis RJ, Mancuso A, Sayed N, Zhang XY, Pfeiffer HK, Nissim I, Daikhin E, Yudkoff M, McMahon SB, and Thompson CB. Myc regulates a transcriptional program that stimulates mitochondrial glutaminolysis and leads to glutamine addiction. PNAS. 2008;105(48):18782–18787.

35. Christensen CE, Karlsson M, Winther JR, Jensen PR and Lerche MH. Non-invasive in-cell determination of free cytosolic [NAD^+]/[NADH] ratios using hyperpolarized glucose show large variations in metabolic phenotypes. J. Biol Chem. 2014;289(4):2344-52.

36. Wasa M, Bode B, Souba WW. Adaptive regulation of amino acid transport in nutrient- deprived human hepatomas. Am J Surg 1996;171:163-169.

37. Perez-Gomez C, Campos-Sandoval JA, Alonso FJ, Segura JA, Manzanares E, Ruiz-Sanchez P, Gonzalez ME, Marquez J, and Mates JM. Co-expression of glutaminase K and L isoenzymes in human tumour cells. Biochem. J. 2005; 386:535–542.

38. Dafni H, Larson PEZ, Hu S, Yoshihara HAI, Ward CS, Venkatesh HS, Wang C, Zhang X, Vigneron DB, Ronen SM. Hyperpolarized 13C spectroscopic imaging informs on hypoxia-inducible factor-1 and Myc activity downstream of platelet-derived growth factor receptor. Cancer Res; 2010, 70(19), 7400-7410.

39. Dafni H and Ronen SM. Dynamic nuclear polarization in metabolic imaging of metastasis: common sense, hypersense and compressed sensing. Cancer Biomark. 2010; 7(4):189-99.

40. Lieberman BP, Ploessl K, Wang L, Qu W, Zha Z, Wise DR, Chodosh LA, Belka G, Thompson CB, Kung HF. PET imaging of glutaminolysis in tumors by 18F-(2S,4R)4-fluoroglutamine. J Nucl Med. 2011; 52(12):1947-55.

Figure captions

Figure 1. Effect of glutamine withdrawal on cell proliferation**.** DU145 and PC3 cells were cultured with (control) or without glutamine ((-) Q) for 4 days. (A-B) Cell counts and (C-D) MTT assays were conducted every 24 h. The data represent means ± SD values from three independent experiments performed in triplicate. Significant differences are indicated by * $P<0.05$.

Figure 2. (A) Real time glutamine metabolism in DU145 cells using hyperpolarized [5-^{13}C]glutamine. **(**B) Single spectrum taken 20 s after start of the experiment shown in A), where [5-^{13}C]glutamate has its maximum. **(**C) Metabolic build-up curves of hyperpolarized [5-^{13}C]glutamate from the 2 cell lines (DU145 and PC3). (D) Area under the curve of the build-up curves from [5-^{13}C]glutamate (n=3). (E) Glutaminase activity measured by RP-HPLC under proliferating conditions. The data represent the mean ± SD from 2 independent experiments performed in triplicate (n=6). Significant difference between DU145 and PC3 cells are indicated by "*" ($P<0.05$).

Figure 3. Effect of resveratrol on survival of prostate cancer cells. (A) DU145 and (B) PC3 cells were treated with resveratrol at indicated concentrations for 24 h in DMEM. At the end of the incubation time, cells were

harvested by trypsinization and were counted. (C-D) Effect of resveratrol on MTT conversion. This assay was evaluated by measuring the amount of formazan crystals after resveratrol exposure in DU145 (C) and PC3 (D) cells. (E-F) Cell lysates were analyzed by nucleosome ELISA in DU145 (E) and PC3 (F) cells. The data represent the means ± SD values from three independent experiments performed in triplicate. Significant differences from control (0.2% DMSO) values are indicated by "*" ($P<0.05$).

Figure 4. Effect of sulforaphane on the survival of prostate cancer cells. (A) DU145 and (B) PC3 cells were treated with sulforaphane at indicated concentrations for 24 h in DMEM. At the end of the incubation time, cells were harvested by trypsinization and were counted. (C-D) Effect of resveratrol on MTT conversion. This assay was evaluated by measuring the amount of formazan crystals after sulforaphane exposure in DU145 (C) and PC3 (D) cells. (E-F) Cell lysates were analyzed by nucleosome ELISA in DU145 (E) and PC3 (F) cells. The data represented the means ± SD values from three independent experiments performed in triplicate. Significant differences from control (0.025% DMSO) are indicated by "*" ($P<0.05$).

Figure 5: (A) Metabolic build-up curves of hyperpolarized [5-^{13}C]glutamate from untreated and treated DU145 cells. **(**B) Area under the curve of the build-up curves from [5-^{13}C]glutamate (n=3) in control and resveratrol treated DU145 cells (200 μM). Glutaminase activity for DU145 and PC3 cells, expressed as mU of glutamate per million cells, measured after 24 h treatment with 200 μM resveratrol. The data represent the mean ± SD from 2 independent experiments performed in triplicate (n=6). Significant difference between untreated vs. treated DU145 is indicated by "*" ($P< 0.05$).

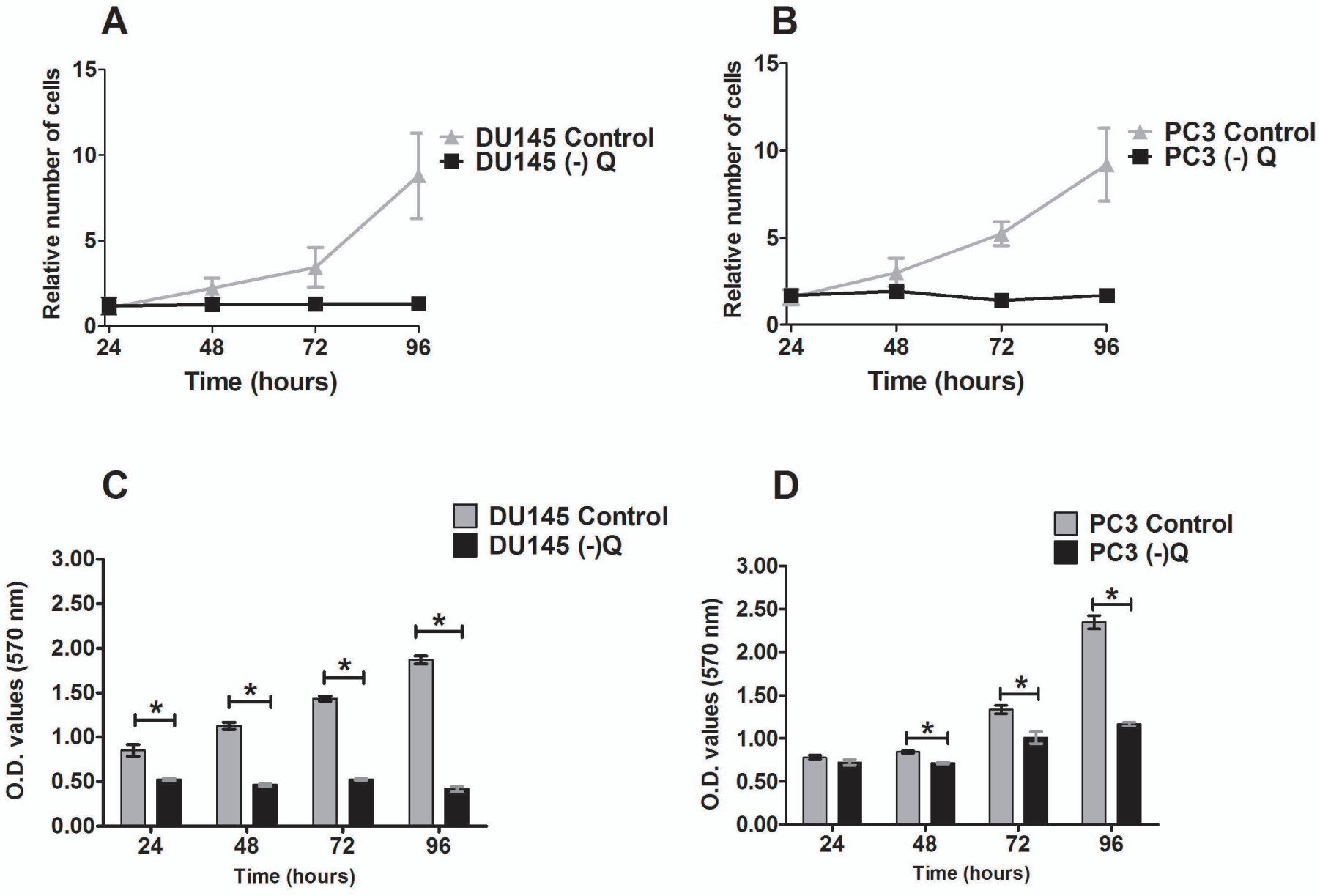
A
Relative number of cells
15
10
5
0
24
48
72
96
Time (hours)
DU145 Control
DU145 (-) Q
B
Relative number of cells
15
10
5
0
24
48
72
96
Time (hours)
PC3 Control
PC3 (-) Q
C
DU145 Control
DU145 (-)Q
O.D. values (570 nm)
3.00
2.50
2.00
1.50
1.00
0.50
0.00
*
24
48
72
96
Time (hours)
D
PC3 Control
PC3 (-)Q
O.D. values (570 nm)
3.00
2.50
2.00
1.50
1.00
0.50
0.00
*
24
48
72
96
Time (hours)

A

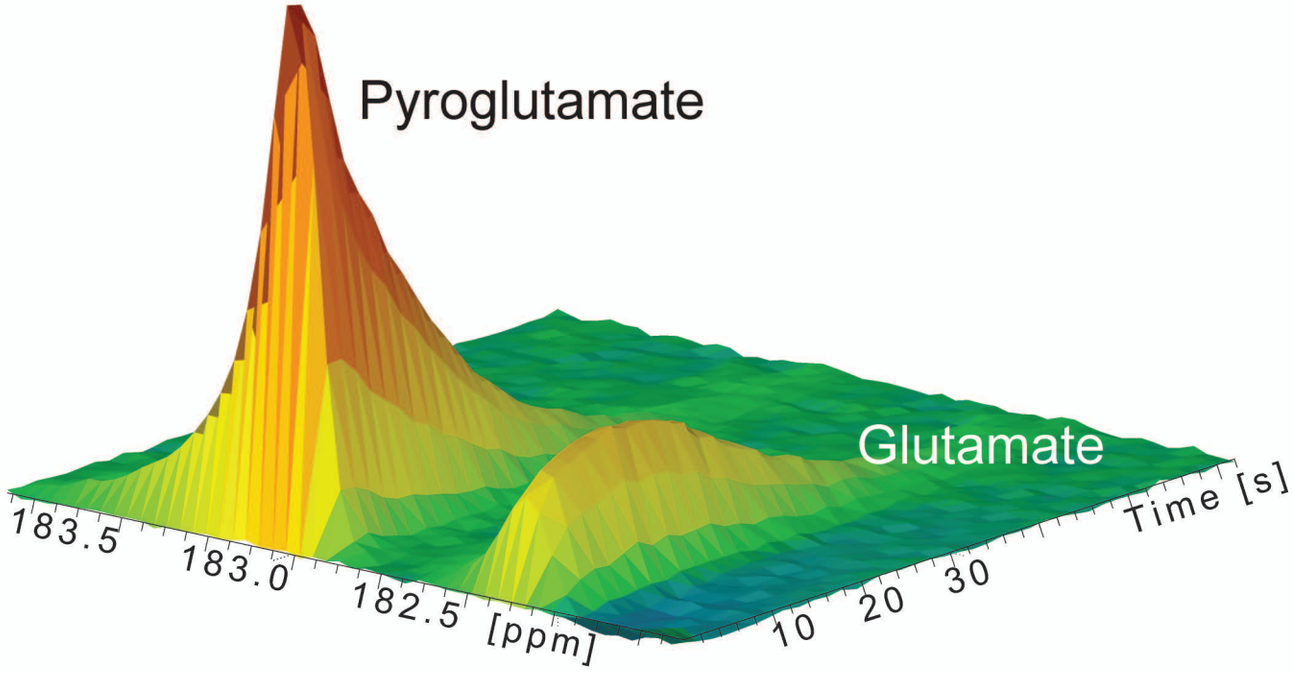
Pyroglutamate
Glutamate
183.5
183.0
182.5
[ppm]
10
20
30
Time [s]

B

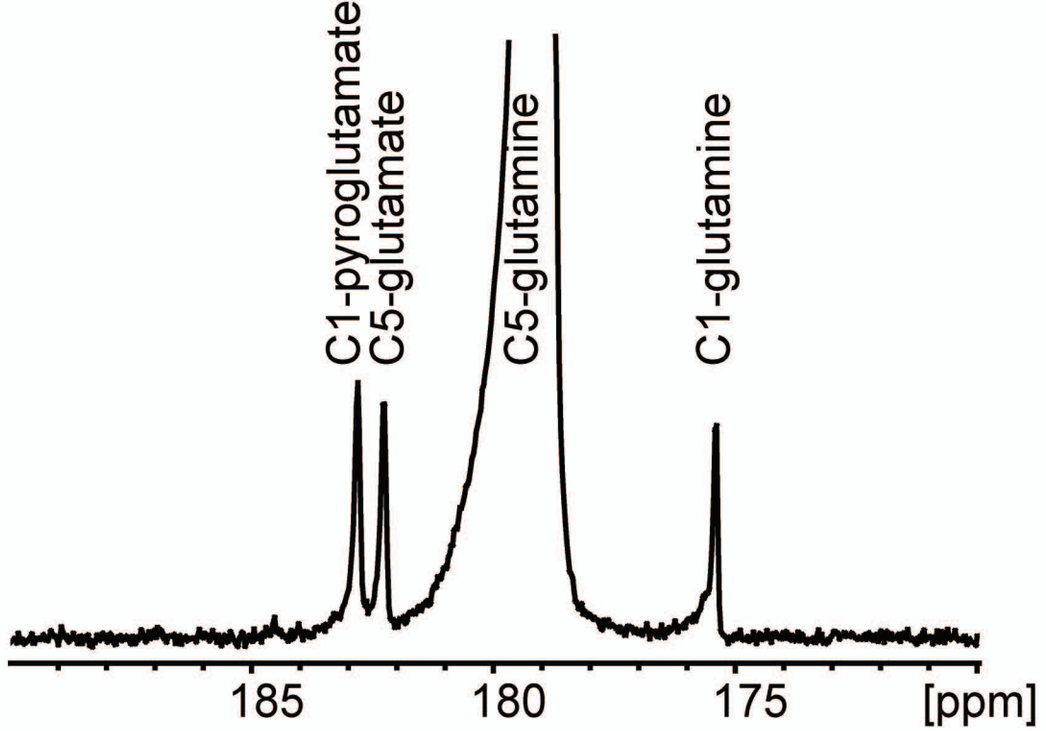
C1-pyroglutamate
C5-glutamate
C5-glutamine
C1-glutamine
185
180
175
[ppm]

C

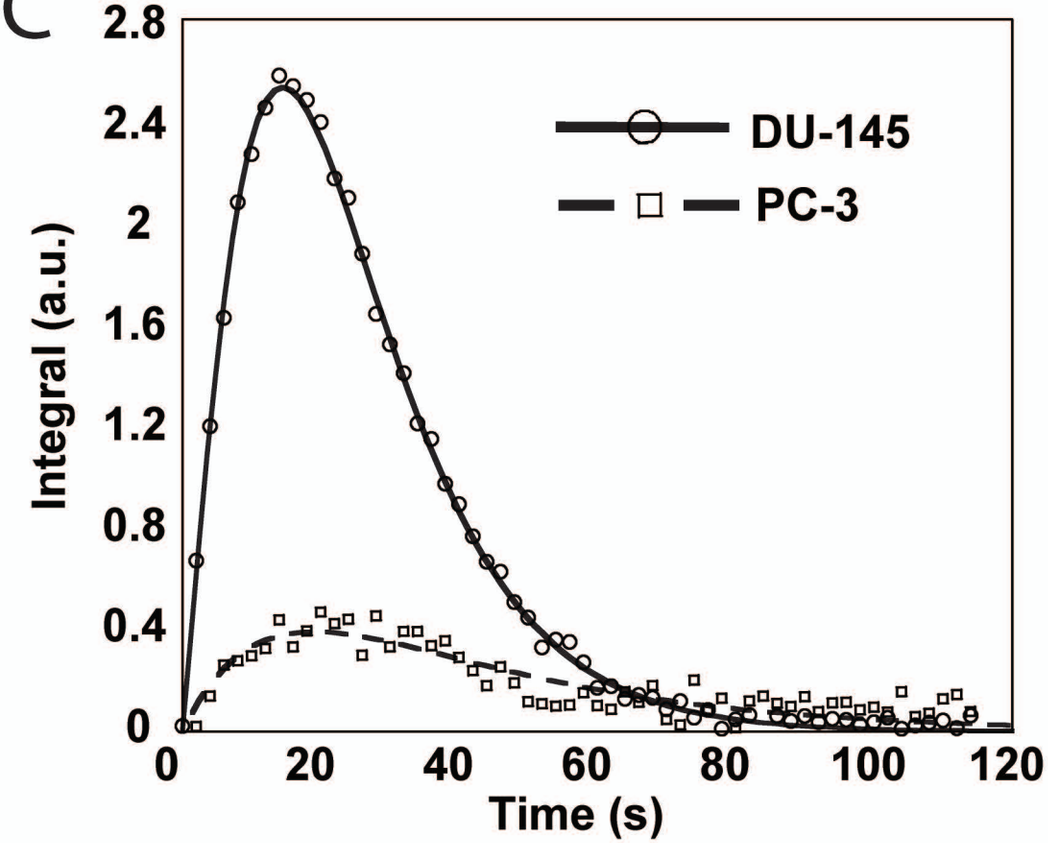
DU-145
PC-3
Integral (a.u.)
Time (s)
0
0.4
0.8
1.2
1.6
2
2.4
2.8
0
20
40
60
80
100
120

D

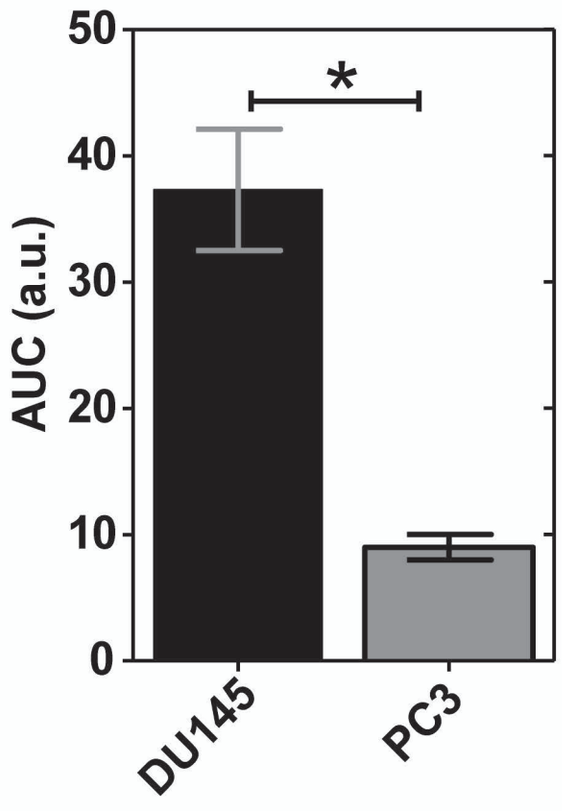
AUC (a.u.)
*
0
10
20
30
40
50
DU145
PC3

E

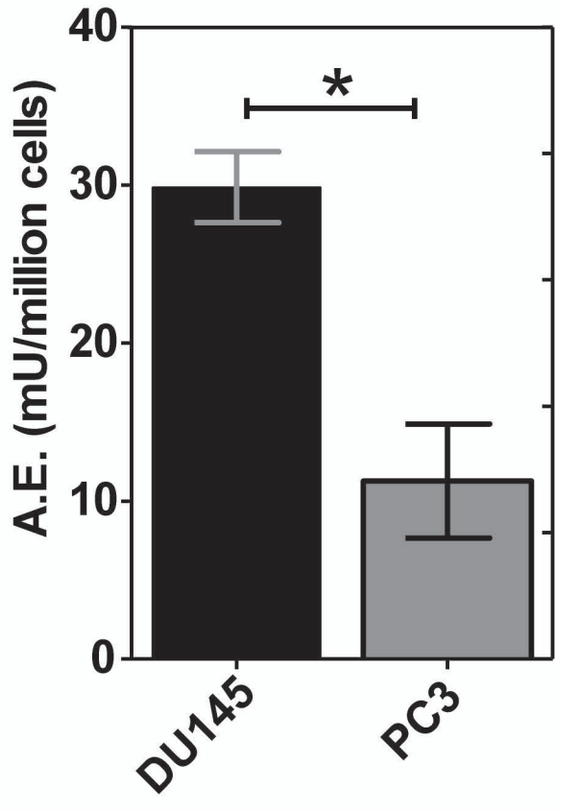
A.E. (mU/million cells)
*
0
10
20
30
40
DU145
PC3

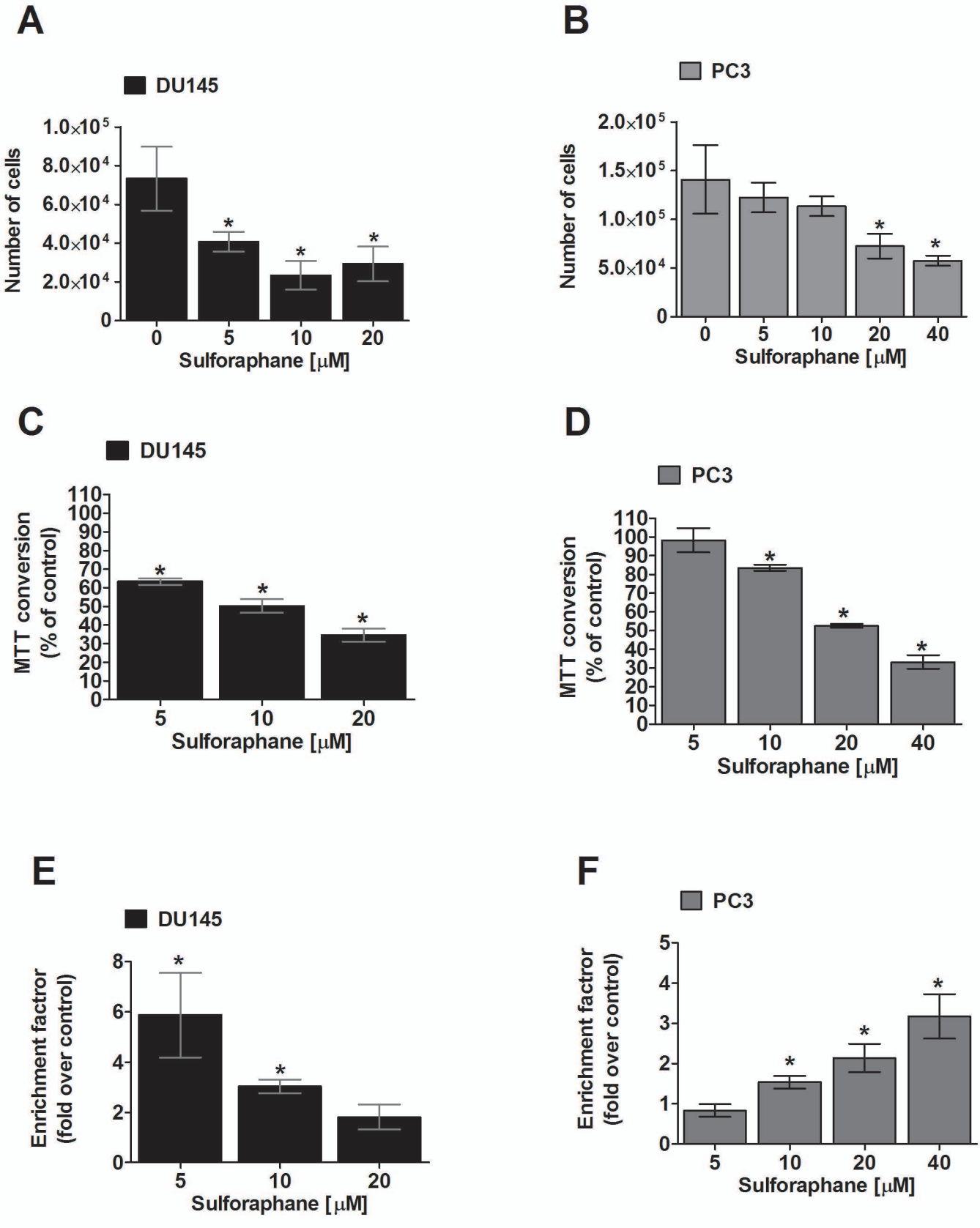
A
DU145
Number of cells
1.0×10^5
8.0×10^4
6.0×10^4
4.0×10^4
2.0×10^4
0
0
5
10
20
Sulforaphane [μM]
B
PC3
Number of cells
2.0×10^5
1.5×10^5
1.0×10^5
5.0×10^4
0
0
5
10
20
40
Sulforaphane [μM]
C
DU145
MTT conversion (% of control)
110
100
90
80
70
60
50
40
30
20
10
0
5
10
20
Sulforaphane [μM]
D
PC3
MTT conversion (% of control)
110
100
90
80
70
60
50
40
30
20
10
0
5
10
20
40
Sulforaphane [μM]
E
DU145
Enrichment factror (fold over control)
8
6
4
2
0
5
10
20
Sulforaphane [μM]
F
PC3
Enrichment factror (fold over control)
5
4
3
2
1
0
5
10
20
40
Sulforaphane [μM]

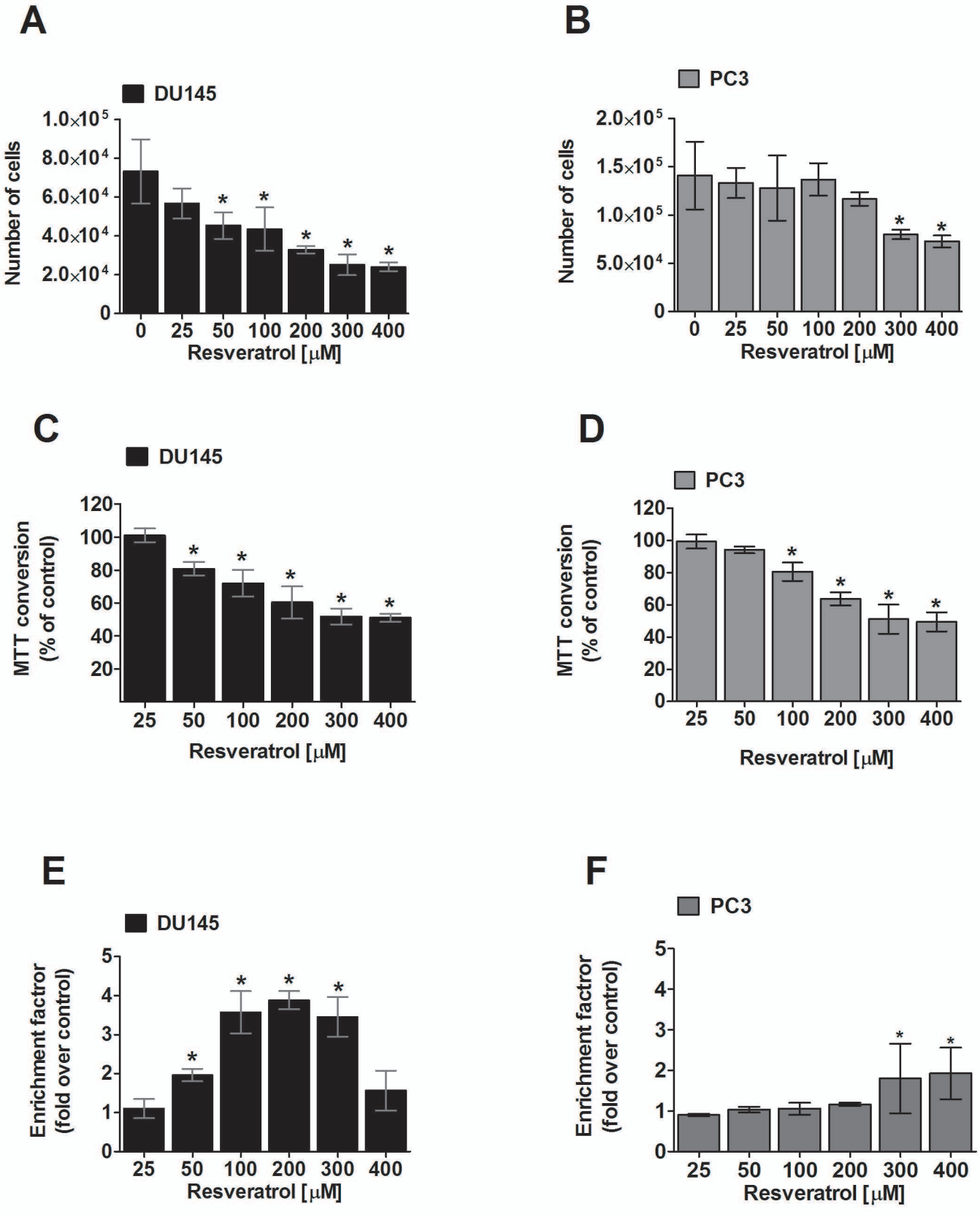
A
DU145
Number of cells
1.0×10^5
8.0×10^4
6.0×10^4
4.0×10^4
2.0×10^4
0
0 25 50 100 200 300 400
Resveratrol [μM]
B
PC3
Number of cells
2.0×10^5
1.5×10^5
1.0×10^5
5.0×10^4
0
0 25 50 100 200 300 400
Resveratrol [μM]
C
DU145
MTT conversion (% of control)
120
100
80
60
40
20
25 50 100 200 300 400
Resveratrol [μM]
D
PC3
MTT conversion (% of control)
120
100
80
60
40
20
0
25 50 100 200 300 400
Resveratrol [μM]
E
DU145
Enrichment factror (fold over control)
5
4
3
2
1
0
25 50 100 200 300 400
Resveratrol [μM]
F
PC3
Enrichment factror (fold over control)
5
4
3
2
1
0
25 50 100 200 300 400
Resveratrol [μM]

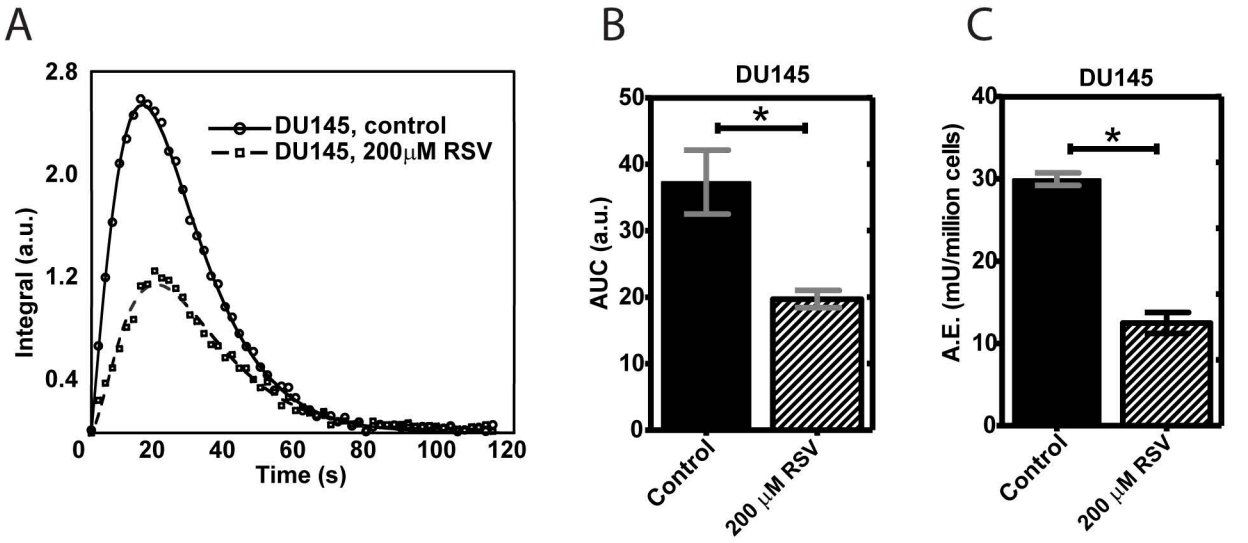
A
2.8
2.0
1.2
0.4
Integral (a.u.)
DU145, control
DU145, 200μM RSV
0
20
40
60
80
100
120
Time (s)
B
DU145
50
40
30
20
10
0
AUC (a.u.)
*
Control
200 μM RSV
C
DU145
40
30
20
10
0
A.E. (mU/million cells)
*
Control
200 μM RSV